Prostaglandin $F_{2\alpha}$ stimulates CFTR activity by PKA- and PKC-dependent phosphorylation

KARIN A. YURKO-MAURO[1] AND WILLIAM W. REENSTRA[2]
Departments of [1]Clinical Science and [2]Pediatrics, Alfred I. duPont Hospital for Children, Thomas Jefferson University, Wilmington, Delaware 19803

Yurko-Mauro, Karin A., and William W. Reenstra. Prostaglandin $F_{2\alpha}$ stimulates CFTR activity by PKA- and PKC-dependent phosphorylation. *Am. J. Physiol.* 275 (*Cell Physiol.* 44): C653–C660, 1998.—The cystic fibrosis transmembrane conductance regulator (CFTR) can be activated by protein kinase A (PKA)- or protein kinase C (PKC)-dependent phosphorylation. To understand how activation of both kinases affects CFTR activity, transfected NIH/3T3 cells were stimulated with forskolin (FSK), phorbol myristate acetate (PMA), or prostaglandin $F_{2\alpha}$ (PGF). PGF stimulates inositol trisphosphate and cAMP production in NIH/3T3 cells. As measured by I^- efflux, maximal CFTR activity with PGF and FSK was equivalent and fivefold greater than that with PMA. Both PGF and PMA had additive effects on FSK-dependent CFTR activity. PMA did not increase cellular cAMP, and maximal PGF-dependent CFTR activity occurred with ~20% of the cellular cAMP observed with FSK-dependent activation. Staurosporine, but not H-89, inhibited CFTR activation and in vivo phosphorylation at low PGF concentrations. In contrast, at high PGF concentrations, CFTR activation and in vivo phosphorylation were inhibited by H-89. As judged by protease digestion, the sites of in vivo CFTR phosphorylation with FSK and PMA differed. For PGF, the data were most consistent with in vivo CFTR phosphorylation by PKA and PKC. Our data suggest that activation of PKC can enhance PKA-dependent CFTR activation.

protein phosphorylation; iodide efflux; phorbol ester; adenosine 3′,5′-cyclic monophosphate; NIH/3T3 cells; chloride channels

CYSTIC FIBROSIS is caused by mutations in the cystic fibrosis transmembrane conductance regulator (CFTR) protein, a Cl^- channel that is activated by ATP hydrolysis and protein kinase A (PKA)-dependent phosphorylation (1, 5, 22). PKA-dependent activation involves phosphorylation of multiple sites within a highly charged intracellular domain, the regulatory or R-domain (5). Mutational analysis suggests that the addition of negative charge induces a conformational change in the R-domain that is necessary for channel activation (9, 21). However, these studies have failed to identify specific phosphorylation sites that are required for CFTR activation and suggest that channel activation is due to a nonlocalized decrease in the net charge of the R-domain. In vivo phosphorylation studies have identified five serines (S660, S700, S737, S795, and S813) as sites of PKA-dependent phosphorylation (5, 19). Mutations at these sites have been shown to alter dose-response curves for agonist-dependent CFTR activation but do not block channel activation (27). In contrast, several kinetic studies have demonstrated functional differences among, as yet unidentified, PKA-dependent phosphorylation sites (12, 13). Together, these data suggest that PKA-dependent CFTR regulation may be more complex than a two-state model.

In addition to PKA-dependent activation, CFTR can also be activated by PKA-independent mechanisms. Several studies have demonstrated protein kinase C (PKC)-dependent CFTR activation and modulation of PKA-dependent activity. In excised patches from transfected Chinese hamster ovary cells, PKC increases the open probability of PKA-activated channels (24). In excised patches from stably transfected NIH/3T3 (NIH-CFTR) cells, PKC activates CFTR to ~20% of the activity obtained with PKA (3). In transfected C127 cells, phorbol myristate acetate (PMA) increases CFTR activity but to levels that are less than those obtained with cAMP-dependent agonists (8). CFTR activation by both PKA and PKC has been observed in cardiac myocytes and in pancreatic acinar cells, but in both systems the effects of CFTR activation with PKA plus PKC has not been described (7, 16). It has also been reported that a basal PKC-dependent phosphorylation is required for PKA-dependent CFTR activity (15). PKC-dependent phosphorylation has been shown to occur at serines 686, 700, and 790 (10, 19). It can be assumed, but has not been demonstrated, that phosphorylation at these sites is required for PKC-dependent alterations to CFTR activity. These results suggest that PKC may modulate PKA-dependent CFTR activation. This modulatory effect may be important under in vivo conditions in which agonists that stimulate both pathways are likely to be present.

To study the effects of the combined activation of PKA and PKC on CFTR activity, we have examined stimulation by prostaglandin $F_{2\alpha}$ (PGF). PGF-dependent stimulation was compared with stimulation with forskolin (FSK) and PMA, activators of PKA and PKC, respectively. In NIH/3T3 cells, PGF increases intracellular Ca^{2+} and inositol trisphosphate (11, 18, 26). It has also been reported, and confirmed in this study, that PGF increases intracellular cAMP in NIH/3T3 cells (11). Thus, in NIH-CFTR cells, PGF provides a model for evaluating the combined effects of PKA and PKC on CFTR activity. PGF caused maximal stimulation of CFTR activity at a level of cellular cAMP that was 25% of that required for maximal stimulation with FSK. PMA increased CFTR activity to ~20% of the maximal activity seen with FSK without increasing cellular cAMP. Both PMA and PGF had additive effects on FSK-dependent CFTR activity. PMA- and PGF-depen-

The costs of publication of this article were defrayed in part by the payment of page charges. The article must therefore be hereby marked "*advertisement*" in accordance with 18 U.S.C. Section 1734 solely to indicate this fact.

Downloaded from journals.physiology.org/journal/ajpcell (065.021.193.086) on March 14, 2022.

dent CFTR activity and phosphorylation were inhibited by PKC antagonists. Phosphopeptide maps of in vivo-phosphorylated CFTR allowed PKA- and PKC-dependent phosphorylation to be distinguished and suggested PGF-dependent activation was due to phosphorylation by both kinases. Our results demonstrate that the combined activation of both signal transduction pathways allows maximal CFTR activation at lower cAMP levels than those required for activation solely by PKA.

METHODS

Cell culture. NIH-CFTR and NIH-mock cells, obtained from Dr. Richard Mulligan, were grown as described previously (2, 14). Briefly, cells were cultured at 37°C with 5% CO_2 in DMEM supplemented with 100 μg/ml penicillin, 50 μg/ml streptomycin, 50 μg/ml gentamicin, and 10% newborn calf serum. For I^- efflux studies, cells were grown on four-well, 15-mm plates. For in vivo phosphorylation and cAMP measurements, cells were grown on 35-mm plates; for peptide mapping, cells were grown on 60-mm plates.

I^- efflux. CFTR activity was assayed by measuring the rate of I^- efflux. Measurements were performed as previously described (14, 25). Cells, at 37°C, were incubated for 30 min with efflux buffer (in mM: 141 NaCl, 3 KCl, 2 KH_2PO_4, 0.9 $MgCl_2$, 1.7 $CaCl_2$, 10 HEPES, and 10 glucose, pH 7.4) containing 5 μCi/ml carrier-free ^{125}I (sodium salt). For studies at 50 mM extracellular K^+, 45 mM NaCl was replaced with KCl. The loss of intracellular ^{125}I was determined by replacing the bathing solution with efflux buffer every 60 s for 10 min. Agonist or vehicle was present at all times after 4 min. When present, *N*-[2-*p*-bromocinnamyl(amino)ethyl]-5-isoquinolinesulfonamide (H-89) was added at the start of the ^{125}I uptake and staurosporine was added at the start of the measured efflux. Intracellular $^{125}I^-$ was calculated at each time point and rates of I^- efflux (r) were determined from $r = \ln(^{125}I_{t_1}/^{125}I_{t_2})/(t_1 - t_2)$, where $^{125}I_{t_1}$ and $^{125}I_{t_2}$ are intracellular ^{125}I at successive time points t_1 and t_2. Rates of I^- efflux were time dependent, and all comparisons were based on maximal values for the time-dependent rates (peak rates). Dose-response curves were obtained by fitting data for peak rates to

$$r = \{V_0 + V_{max}([Ag]/K_a)\}/\{1 + ([Ag]/K_a)\}$$

where V_0 and V_{max} are the rates at 0 and infinite agonist concentration, [Ag] is the concentration of agonist, and K_a is the agonist concentration that gives a half-maximal change. Nonlinear least squares regression was performed with software from Jandel Scientific.

Measurement of cellular cAMP. Cellular cAMP was determined by radioimmunoassay using a commercial kit (Amersham). Samples were prepared as recommended by the manufacturer. Briefly, confluent NIH-CFTR cells were preincubated for 10 min at 37°C with phosphate-free efflux buffer (in mM: 141 NaCl, 5 KCl, 0.9 $MgCl_2$, 1.7 $CaCl_2$, 10 HEPES, and 25 glucose, pH 7.4). Cells were stimulated with agonist for 2 min, and the reaction was terminated by removing the buffer and adding 500 μl of 70% ethanol at 4°C. Cells were collected and centrifuged at 2,000 *g* for 15 min, and the supernatant was recovered. Cells were reextracted with ethanol. The supernatants were combined and evaporated overnight at 70°C. The residue was dissolved in 600 μl of 50 mM sodium acetate, pH 5.8, and cAMP concentrations were determined by radioimmunoassay. cAMP levels were normalized to total cell protein determined by bicinchoninic acid (BCA) assay (23).

In vivo CFTR labeling with $^{32}P_i$. In vivo CFTR labeling was performed as previously described (20). Cells were incubated for 90 min in phosphate-free efflux buffer containing 0.4 mCi/ml [^{32}P]orthophosphate (3,000 Ci/mmol). Cells were washed with phosphate-free efflux buffer and stimulated with agonist for 2 min. When present, H-89 was added to the ^{32}P buffer for the final 30 min and was present during treatment with agonist; staurosporine was added with agonist. After stimulation, cells were lysed with 4°C RIPA buffer (100 mM NaCl, 50 mM NaF, 0.1% SDS, 1% sodium deoxycholate, 1% Triton X-100, 1 mM EDTA, 1 mM EGTA, 0.1 mM PMSF, 0.1 mg/ml aprotinin, 1 mM orthovanadate, and 50 mM Tris·HCl, pH 7.5). Lysates were cleared by centrifugation (100,000 *g* for 20 min), and CFTR immunoprecipitated from 1.7 mg/ml supernatant with 2 μg/ml CFTR monoclonal antibody (MAb; Genzyme, anti-COOH-terminal). CFTR was resolved by SDS-PAGE, visualized by autoradiography, and quantified by scintillation counting of excised bands. For two-dimensional (2-D) phosphopeptide mapping, cells were incubated for 150 min with phosphate-free buffer containing 2 mCi/ml [^{32}P]orthophosphate (3,000 Ci/mmol), and cleared lysates (3.8 mg/ml) were incubated with 7.5 μg/ml anti-CFTR MAb. Protein was determined by BCA assay.

Staphylococcus aureus V8 protease digestion. V8 Protease digestion was performed as described previously (6, 20). Immunoprecipitated CFTR was excised from gels and placed into the wells of 20% acrylamide gels with 2.5 units of *Staphylococcus aureus* V8 protease (Sigma). SDS sample buffer supplemented with 1 mM EDTA was added, and samples were run into the stacking gel and digested for 2 h. The peptides were then separated by electrophoresis, and labeled peptides were visualized by autoradiography.

Tryptic digestion and 2-D peptide mapping. 2-D phosphopeptide mapping of in vivo-labeled CFTR was performed as described previously (4). After separation by SDS-PAGE, gel slices containing ^{32}P-labeled CFTR were rehydrated and suspended in 50 mM NH_4HCO_3 (pH 7.4) containing 0.1% SDS and 5% β-mercaptoethanol. BSA (20 μg) was added to the clarified supernatant, and protein was precipitated with 17% TCA. Pellets were washed with 100% ethanol, suspended in 50 mM NH_4HCO_3, and digested for 16 h at 37°C with 25 units *N*-tosyl-L-phenylalanine chloromethyl ketone (TPCK)-trypsin (Worthington). An additional 25 units of TPCK-trypsin were added, and the digestion continued for 2 h. Samples were diluted with water and lyophilized to dryness four times. Peptides were then spotted onto 20 × 20-cm TLC plates (EM Science), separated by electrophoresis for 30 min at 1,000 V in 100 mM $(NH_4)_2CO_3$, pH 8.9, and followed by ascending chromatography in *n*-butanol-pyridine-water-acetic acid, 15:10:12:3 (vol/vol/vol/vol). Phosphopeptides were detected with the Storm 860 PhosphorImager (Molecular Dynamics) and identified by comparison with previously published studies (5) and maps provided by Dr. Jonathan Cohn.

Materials. PGF was obtained from Sigma and dissolved in 100% ethanol; the final ethanol concentration in all buffers was ≤0.1%. FSK, PMA, H-89, and staurosporine were obtained from Alexis. Stock solutions were dissolved in DMSO so that the final concentration of DMSO in all buffers was ≤0.2%. Radiochemicals were obtained from DuPont NEN.

Statistics. Calculated values are presented as means ± SE. Comparisons were made among paired data by Student's *t*-test, with $P < 0.05$ taken as significant.

RESULTS

CFTR activation by FSK and PGF. Kinase-dependent CFTR activation was investigated by assaying I^- efflux and in vivo CFTR phosphorylation in NIH-CFTR cells.

Downloaded from journals.physiology.org/journal/ajpcell (065.021.193.086) on March 14, 2022.

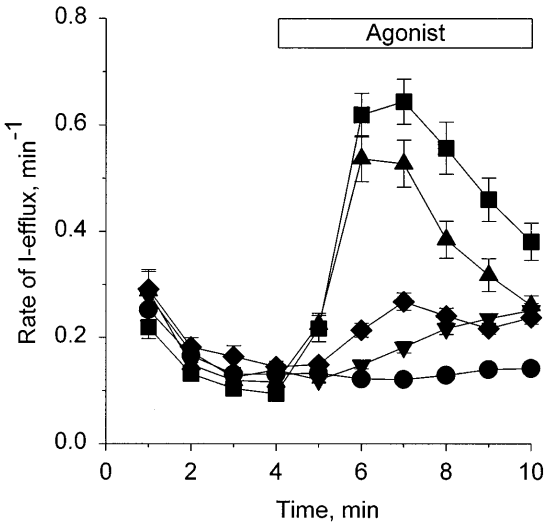

Fig. 1. Time courses for agonist-stimulated I^- efflux in NIH-CFTR cells. Confluent monolayers at 37°C were loaded with ^{125}I for 30 min, extracellular ^{125}I was removed, and I^- efflux was assayed by changing bathing medium every 60 s for 10 min. Rates were calculated as described in METHODS. Agonists [1.0 μM forskolin (FSK, ■), 1.0 μM prostaglandin $F_{2\alpha}$ (PGF, ▲), 0.01 μM PGF (◆), 200 nM phorbol myristate acetate (PMA, ▼), or vehicle (0.2% DMSO) (●)] were present in bathing medium where indicated by bar. Data are means ± SE [no. of experiments (n) ≥ 15].

As shown in Fig. 1, the addition of agonist caused a time-dependent increase in the rate of I^- efflux. A transient increase in the rate of I^- efflux with a peak rate 2–3 min after agonist addition was observed with FSK and with PGF. With PMA, a more gradual increase in the rate of I^- efflux was observed. Mean values for peak rates of I^- efflux were 0.64 ± 0.04 min^{-1} [no. of experiments (n) = 15] for 1 μM FSK, 0.25 ± 0.01 min^{-1} (n = 16) for 200 nM PMA, 0.54 ± 0.04 min^{-1} (n = 16) for 1 μM PGF, and 0.27 ± 0.02 min^{-1} (n = 16) for 0.01 μM PGF. Mean rates in the absence of agonist were 0.12 ± 0.01 min^{-1} (n = 15). Two tests were performed to determine if PGF-dependent I^- efflux was due to stimulation of CFTR or another anion channel. *1*) I^- efflux was assayed in mock-transfected NIH/3T3 (NIH-mock) cells. In NIH-mock cells, the average rate of I^- efflux was 0.16 min^{-1} (n = 2) in the absence of agonist. Peak rates in the presence of 1 μM PGF and 1 μM FSK were on average 0.18 min^{-1} (n = 2) and 0.17 min^{-1} (n = 2), respectively; neither agonist caused a significant increase. *2*) In NIH-CFTR cells, I^- efflux was assayed in the presence of dinitrostilbene-2–2′-disulfonic acid (DNDS), a nonspecific Cl^- channel inhibitor that does not inhibit CFTR from the extracellular side (17). Peak rates of I^- efflux in the absence of DNDS were 0.49 ± 0.03 min^{-1} (n = 3) for 1 μM FSK and 0.70 ± 0.08 min^{-1} (n = 4) for 1 μM PGF. In the presence of 100 μM DNDS, peak rates were 0.63 ± 0.02 min^{-1} (n = 3) for 1 μM FSK and 0.76 ± 0.05 min^{-1} (n = 4) for 1 μM PGF. Together, these results demonstrate that the PGF-dependent increases in I^- efflux reflect CFTR activation.

Although these results demonstrate PGF-dependent CFTR activation, PGF-dependent activation of a K^+ conductance could increase the membrane potential and thereby increase the rate of CFTR-dependent I^- efflux. To determine if an increase in K^+ conductance contributed to the PGF-dependent increase in I^- efflux, rates of I^- efflux were measured in the presence of 5 and 50 mM extracellular K^+. If, in the presence of 5 mM extracellular K^+, K^+ channel activation increased I^- efflux by hyperpolarizing the membrane potential, K^+ channel activation with 50 mM extracellular K^+ would depolarize the membrane potential and inhibit the rate of I^- efflux. At 50 mM K^+, the rates of I^- efflux as a percentage of those with 5 mM K^+ were 92 ± 11% (n = 3) with 1 μM FSK and 112 ± 3% (n = 4) with 1 μM PGF. Because PGF-stimulated I^- efflux was not reduced with 50 mM extracellular K^+, a PGF-dependent hyperpolarization of the membrane potential is unlikely to contribute to the observed PGF-dependent rate of I^- efflux.

The dose-response relationship for PGF-dependent activation of I^- efflux was examined. As shown in Fig. 2, a maximal rate of I^- efflux was seen at 1 μM PGF with an EC_{50} of 50 ± 10 nM. Additive effects of PMA and PGF on FSK-dependent CFTR activity were observed. As shown in Fig. 3, rates of I^- efflux with saturating concentrations of PGF and FSK (14) were similar [0.66 ± 0.03 min^{-1} (n = 7) and 0.74 ± 0.04 min^{-1} (n = 7), respectively]. However, in the presence of both agonists, the rate of I^- efflux, 1.06 ± 0.04 min^{-1} (n = 7), was significantly greater than that with either agonist alone. A similar additive effect on FSK-dependent I^- efflux was produced with PMA.

To determine if CFTR activation by PGF involved the activation of PKC, the effects of the PKA- and PKC-selective inhibitors, H-89 and staurosporine, on agonist-dependent I^- efflux were determined. In Fig. 4, rates of agonist-dependent I^- efflux were plotted after subtraction of control rates in the absence of agonist. For each agonist, data are presented without inhibitor, with 10 μM H-89, and with 1 μM staurosporine. Neither inhibitor had a significant effect on the control rate of I^- efflux (data not shown). PMA-dependent I^- efflux was significantly inhibited by staurosporine by 57 ± 6% (n = 6) but was not inhibited by H-89. A similar pattern was observed with 0.01 μM PGF, in which staurosporine

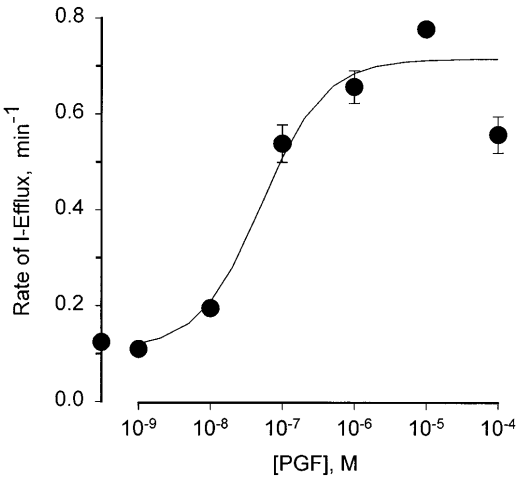

Fig. 2. Dose-response relationship for PGF-stimulated I^- efflux in NIH-CFTR cells. I^- efflux was assayed as described in Fig. 1, and peak rates were plotted as a function of PGF concentration. Data are means ± SE (n ≥ 2). The line was fit by nonlinear least squares regression.

Downloaded from journals.physiology.org/journal/ajpcell (065.021.193.086) on March 14, 2022.

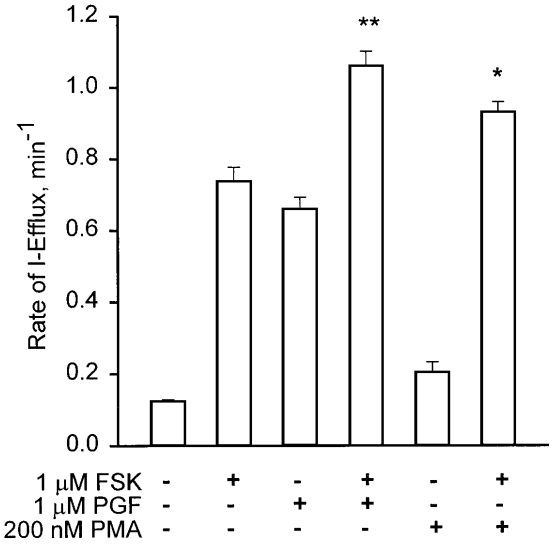

Fig. 3. Additive effects of PGF and PMA on FSK-dependent I^- efflux in NIH-CFTR cells. I^- efflux was assayed as described in Fig. 1, and peak rates for the indicated agonists are plotted as means ± SE ($n \geq 7$). Rates in the presence of 1.0 μM PGF plus 1.0 μM FSK were significantly greater than those for 1.0 μM PGF or 1.0 μM FSK alone, $^{**}P \leq 0.01$. Rates in the presence of 200 nM PMA plus 1.0 μM FSK were significantly greater than those for 200 nM PMA or 1.0 μM FSK alone, $^{*}P \leq 0.05$.

inhibited I^- efflux by 31 ± 6% ($n = 8$), whereas H-89 had no effect. In contrast, FSK-dependent I^- efflux was significantly inhibited by H-89, 30 ± 4% ($n = 5$), but not by staurosporine. A similar pattern was observed with 1.0 μM PGF: H-89 inhibited I^- efflux by 76 ± 5% ($n = 3$), whereas staurosporine had no effect. These results suggest that, at low PGF concentrations, PGF-dependent I^- efflux involves activation of PKC, whereas, at high concentrations, a PKA-dependent pathway may be involved in channel activation.

Agonist-stimulated cAMP levels. The role of PKA in PGF-dependent CFTR activation was also assessed by comparing cAMP levels and rates of I^- efflux. In Fig. 5, rates of PGF- and FSK-dependent I^- efflux were plotted against cAMP levels obtained under the same experimental conditions. For both PGF and FSK, rates of I^- efflux were increased when cAMP levels increased, but the slope of the regression line for PGF (54 ± 15 $min^{-1} \cdot nmol^{-1} \cdot mg$) was significantly greater ($P < 0.01$) than that for FSK (8.0 ± 0.07 $min^{-1} \cdot nmol^{-1} \cdot mg$). Thus, at comparable levels of cAMP, PGF produced a greater increase in channel activity. Two explanations are possible for this result. PGF may stimulate a localized production of cAMP that is tightly coupled to PKA-dependent stimulation of CFTR, whereas FSK increases cAMP levels throughout the cell. This would require a higher level of total cAMP with FSK than with PGF to achieve the same amount of PKA-dependent CFTR activity. Alternatively, PGF may activate a cAMP-independent pathway that enhances PKA-dependent CFTR activation.

To determine if PKC enhanced PKA-dependent CFTR activation without increasing cAMP levels, I^- efflux and cAMP were measured during stimulation with 200 nM PMA and with 200 nM PMA plus 0.1 μM FSK. In both cases, PMA produced a significant increase in channel activity with no significant increase in cAMP (Fig. 5). In a similar fashion, 0.01 μM PGF produced a significant increase in channel activity with no increase in cAMP levels. These results demonstrate that, in addition to enhancing PKA-dependent channel activation (Fig. 3), PKC can stimulate CFTR without increasing cAMP levels. They also suggest that PGF-dependent CFTR activation might involve the activation of PKC.

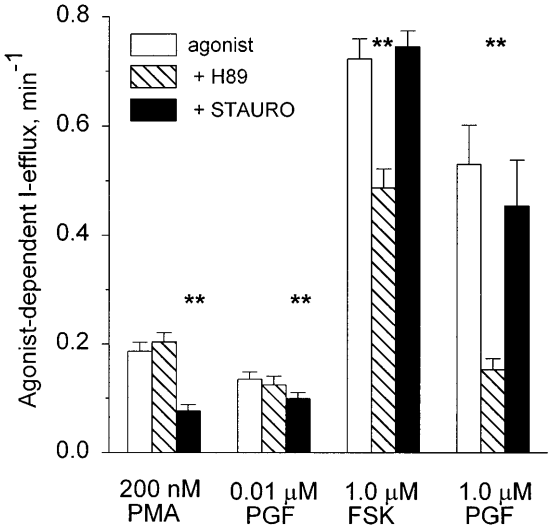

Fig. 4. Inhibition of agonist-dependent I^- efflux by H-89 and staurosporine (stauro). Rates of I^- efflux were assayed with indicated agonists in the absence (open bars) and presence of 10 μM H-89 or 1.0 μM staurosporine. In all cases, paired control rates in the absence of agonist (0.128 ± 0.005 min^{-1}) were subtracted from rates in the presence of agonist; neither H-89 nor staurosporine had any effect on the control rate. Data are means ± SE ($n \geq 3$). Where indicated (**), rates in the presence of inhibitor were significantly less ($P \leq 0.01$) than the uninhibited rate.

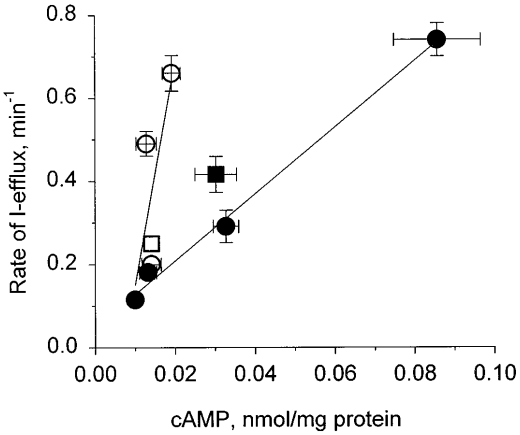

Fig. 5. Dependence of agonist-stimulated I^- efflux on intracellular cAMP. Rates of I^- efflux were assayed as described in Fig. 1, and peak rates were determined. In parallel experiments, cAMP levels were assayed by radioimmunoassay. Rates of I^- efflux with 0, 0.01, 0.1, and 1.0 μM FSK (●); 0.01, 0.1, and 1.0 μM PGF (○); 200 nM PMA (□); and 200 nM PMA plus 0.1 μM FSK (■) were plotted as a function of intracellular cAMP. Data for both I^- efflux and cAMP are means ± SE ($n \geq 6$). Lines for FSK and PGF were obtained by linear regression; slopes were significantly different at $P \leq 0.01$.

Downloaded from journals.physiology.org/journal/ajpcell (065.021.193.086) on March 14, 2022.

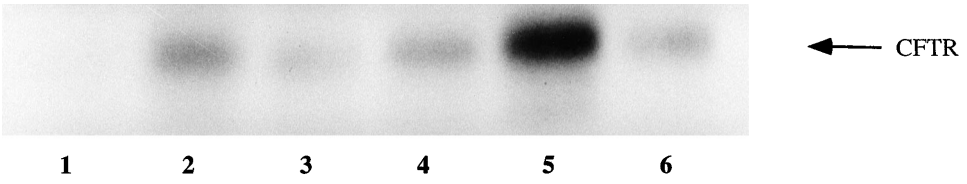

Fig. 6. Agonist-dependent in vivo CFTR phosphorylation in NIH-CFTR cells. Agonist-dependent in vivo phosphorylation and immunoprecipitation were performed as described in METHODS. CFTR was resolved by SDS-PAGE and detected by autoradiography. In the representative autoradiogram, cells were stimulated with no agonist (*lane 1*), 1.0 μM FSK (*lane 2*), 0.01 μM PGF (*lane 3*), 1.0 μM PGF (*lane 4*), 1.0 μM PGF plus 1.0 μM FSK (*lane 5*), and 200 nM PMA (*lane 6*). Data are representative of 3 experiments.

In vivo CFTR phosphorylation. To further examine PGF-dependent CFTR activation, agonist-dependent in vivo phosphorylation was assayed. A representative autoradiogram of in vivo-phosphorylated CFTR that was immunoprecipitated and then resolved by gel electrophoresis is shown in Fig. 6. Relative to control (*lane 1*), CFTR phosphorylation was increased 3.7-fold with 1 μM FSK (*lane 2*), 2-fold with 0.01 μM PGF (*lane 3*), 3-fold with 1 μM PGF (*lane 4*), and 1.6-fold with 200 nM PMA (*lane 6*). In the presence of 1 μM PGF plus 1 μM FSK (*lane 5*), CFTR phosphorylation was 5.7-fold greater than that of the control. To determine the roles of PKA and PKC in PGF-dependent CFTR phosphorylation, agonist-dependent phosphorylation was assayed in the presence of 10 μM H-89 or 1 μM staurosporine. In general, inhibitor-dependent decreases in CFTR phosphorylation were smaller than decreases in I^- efflux. As shown in Fig. 7, PMA-dependent phosphorylation was significantly inhibited by staurosporine (38 ± 5%, n = 5) but not by H-89. A similar pattern was observed with 0.01 μM PGF, in which staurosporine inhibited CFTR phosphorylation by 27 ± 6% (n = 4), whereas H-89 had no effect. In contrast, FSK-dependent phosphorylation was significantly inhibited by H-89 by 31 ± 11% (n = 6) but not by staurosporine. For 1 μM PGF, H-89 inhibited phosphorylation by 16 ± 5% (n = 4), whereas 1 μM staurosporine was without effect. At 10 μM, staurosporine decreased 1 μM PGF-stimulated phosphorylation by 43 ± 16% (n = 3) (data not shown).

V8 protease and trypsin digests of in vivo-phosphorylated CFTR. The sites of in vivo CFTR phosphorylation were examined to determine if channel activation with PMA or PGF was due to phosphorylation by kinases other than PKA. The purpose of these studies was not to identify specific phosphorylation sites but to determine if the pattern of phosphorylation with these agonists differed from FSK. In an initial study, in vivo-phosphorylated CFTR was immunoprecipitated and resolved by electrophoresis before digestion with *Staphylococcus aureus* V8 protease. After digestion, the resulting peptides were separated by electrophoresis. Figure 8 shows a representative autoradiogram of the resolved phosphopeptides. Treatment of cells with agonist produced three prominent phosphopeptides of molecular masses of 17.8, 13.3, and 9 kDa. An additional phosphopeptide with a molecular mass of ~16 kDa was seen when cells were stimulated with PMA or PGF (*lanes 2–5*). Although the 16-kDa band was most clearly seen with PMA (*lane 4*), the band was seen in all lanes in which cells were treated with PGF (*lanes 2*, *3*,

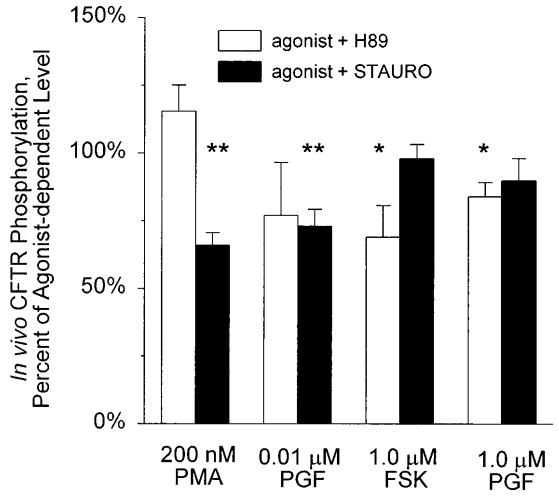

Fig. 7. Inhibition of agonist-dependent in vivo CFTR phosphorylation by H-89 and staurosporine. Agonist-dependent CFTR phosphorylation was assayed with the indicated agonists in the absence and presence of 10 μM H-89 (open bars) or 1.0 μM staurosporine (solid bars). Data are expressed as a percentage of the uninhibited value for each agonist. Data are means ± SE ($n \geq 3$). Statistically significant inhibitions at $P \leq 0.05$ (*) and $P \leq 0.01$ (**) are indicated.

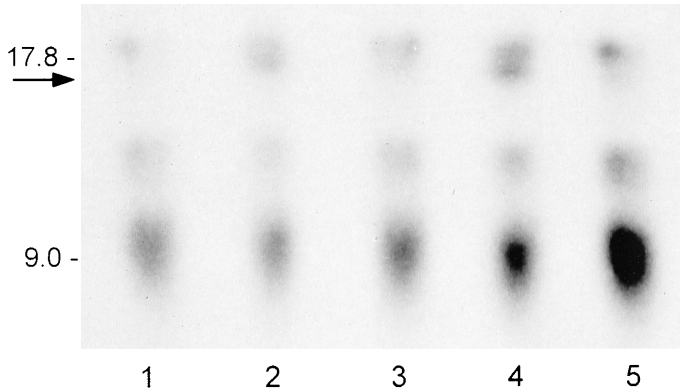

Fig. 8. *Staphylococcus aureus* V8 protease digest of in vivo phosphorylated CFTR. In vivo phosphorylated CFTR, isolated by immunoprecipitation and gel electrophoresis, was digested with V8 protease, and the resulting peptides were resolved by SDS-PAGE. Phosphorylated peptides were observed by autoradiography. In the typical autoradiogram, CFTR was stimulated with 1 μM FSK (*lane 1*), 0.01 μM PGF (*lane 2*), 1 μM PGF (*lane 3*), 200 nM PMA (*lane 4*), and 1 μM PGF + 1 μM FSK (*lane 5*). Molecular mass markers are indicated, and position of a phosphopeptide observed after stimulation with PMA or PGF, but not with FSK, is indicated by arrow. Data are representative of 3 experiments.

Downloaded from journals.physiology.org/journal/ajpcell (065.021.193.086) on March 14, 2022.

and *5*) and not in the lane in which cells were treated with FSK (*lane 1*). None of these phosphopeptides is thought to be degradation products of another phosphopeptide, because the peptide patterns were not altered by changes in the concentration of protease or the length of digestion (W. W. Reenstra and S. Raman, unpublished observations). These results suggest that PMA and PGF stimulate CFTR phosphorylation on at least one site that is not phosphorylated with PKA. Because the additional peptide observed with PMA and PGF appears to have the same molecular mass, the data suggest that PGF activates PKC-dependent phosphorylation.

To confirm the results obtained with V8 protease, in vivo phosphorylated CFTR was also subjected to tryptic digestion and 2-D peptide mapping. In Fig. 9, representative 2-D phosphopeptide maps are shown for in vivo phosphorylated CFTR after stimulation with 1 μM FSK (*A*), 200 nM PMA (*B*), 0.01 μM PGF (*C*), and 1 μM PGF (*D*). Although more than 10 phosphopeptides were resolved, four (phosphopeptides 1–4) were highly phosphorylated and showed agonist-specific differences. In the absence of added agonist (data not shown), there was little phosphorylation of these peptides. CFTR activation with FSK caused peptides 1 and 2 to become highly phosphorylated. On the basis of previously published phosphopeptide maps, phosphopeptides 1 and 2 were assigned to tryptic peptides containing S737 and S795, respectively (5). Previous studies have shown FSK-dependent phosphorylation of these serines as well as S660, S700, and S813 (10). In our studies, S813 (peptide 5) was not heavily phosphorylated and we did not observe phosphopeptides containing S660 and S700. On the basis of previously published maps, the phosphopeptide containing S660 should be below the phosphopeptide containing S795 and the phosphopeptide containing S700 should be to the left of that containing S795. In contrast to stimulation with FSK, stimulation with PMA (Fig. 9*B*) led to high levels of phosphorylation on peptides 1 and 2 and on peptides 3 and 4. Phosphopeptide 3 could contain S768, but we have been unable to identify phosphopeptide 4. With FSK-dependent stimulation, phosphopeptides 3 and 4 were phosphorylated to far lower levels than phosphopeptides 1 and 2. Irrespective of the identification of phosphopeptides 3 and 4, the increased phosphorylation of peptides 3 and 4, relative to that of peptides 1 and 2, was taken as a hallmark of PKC-dependent CFTR phosphorylation. As shown in Fig. 9, *C* and *D*, at both low and high PGF concentrations, peptides 1–4 were phosphorylated. These patterns are clearly different from that with FSK and resemble that with PMA. This suggests that PGF-dependent CFTR stimulation involves phosphorylation by PKC. However, these data do not rule out PGF-dependent CFTR phosphorylation by PKA but, when combined with the inhibitor studies at high PGF concentrations (Figs. 4 and 7), are most consistent with PGF-dependent CFTR activation involving CFTR phosphorylation by both kinases.

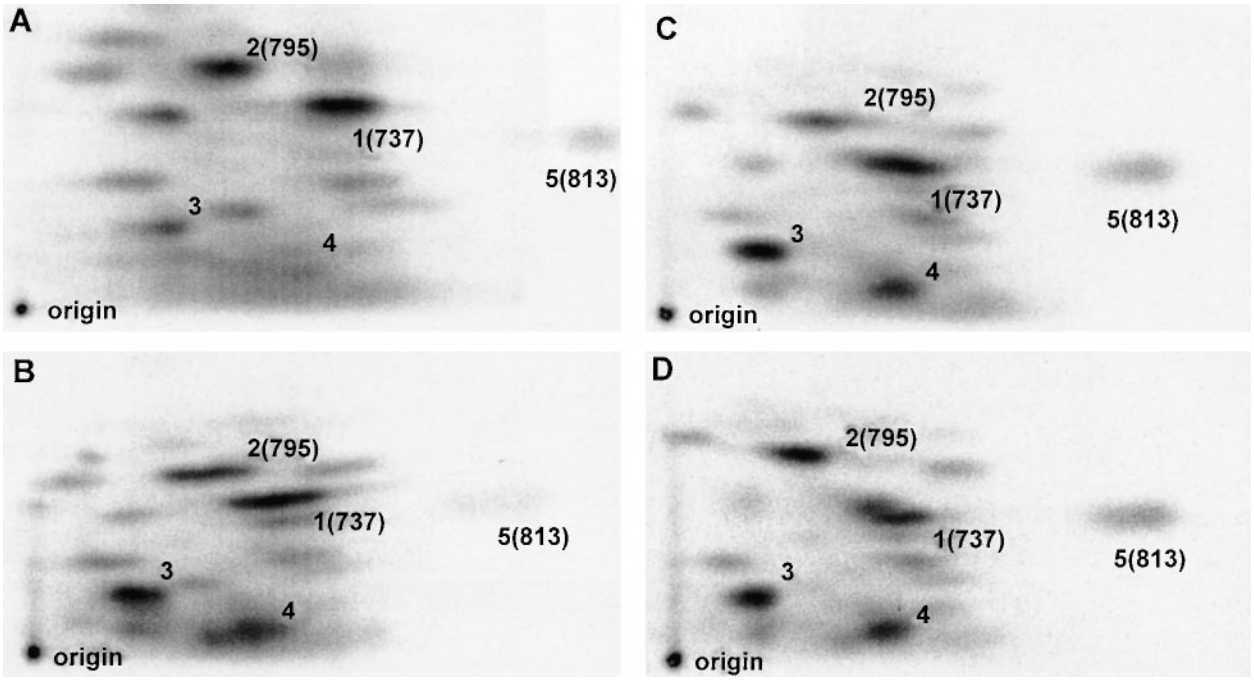

Fig. 9. Two-dimensional (2-D) phosphopeptide maps of tryptic digestion of in vivo phosphorylated CFTR. In vivo phosphorylated CFTR, isolated by immunoprecipitation and gel electrophoresis, was digested with trypsin, and resulting peptides were separated by electrophoresis and ascending chromatography. Phosphopeptides were identified with a Storm 860 PhosphorImager (Molecular Dynamics). Peptide maps of CFTR stimulated with 1 μM FSK (*A*), 200 nM PMA (*B*), 0.01 μM PGF (*C*), and 1 μM PGF (*D*) are shown. Phosphopeptides (1–5) and origin are indicated on each map, with protein kinase A phosphorylation sites indicated. Data are representative of 3 experiments.

Downloaded from journals.physiology.org/journal/ajpcell (065.021.193.086) on March 14, 2022.

DISCUSSION

CFTR is activated by PKA-dependent phosphorylation, and there is growing evidence for PKC-dependent activation (7, 8, 15, 16, 24). In this study, we have attempted to determine if, under in vivo conditions, PKC can modulate PKA-dependent CFTR activation. In addition to examining the effects of FSK and PMA on CFTR activity, we examined the effects of an endogenous agonist, PGF. The studies were carried out in transfected NIH/3T3 cells, a cell line in which PGF stimulates both adenylate cyclase (11) and phospholipase C (11, 18, 26). We have confirmed that PGF stimulates adenylate cyclase, a result that was not observed by a recent study (26). It is not known if PGF stimulates both signal transduction pathways by binding to two distinct receptors or if both signal transduction pathways are coupled to a single receptor. Irrespective of this, PGF is a physiological agonist that may use both PKA- and PKC-dependent signal transduction pathways to activate CFTR.

Previous studies in excised patches have demonstrated that PKC-dependent phosphorylation activates CFTR and has an additive effect on PKA-dependent channel activity (3, 24). Under in vivo conditions, PMA stimulates CFTR in transfected C127 cells, cardiac myocytes, and pancreatic acinar cells (7, 8, 16). Our studies demonstrate that, under in vivo conditions, PKC phosphorylates and activates CFTR. In addition, we demonstrate that in vivo phosphorylation by PKC has an additive effect on PKA-dependent CFTR activity. Our results also suggest that PGF-dependent CFTR activation involves the stimulation of both PKA- and PKC-dependent signal transduction pathways.

Our work shows that PGF stimulates CFTR and that the increase in CFTR activity for a given level of cellular cAMP is greater with PGF than with FSK. Several explanations are possible for this finding. *1*) PGF, as opposed to FSK, might increase the membrane potential, thereby increasing the rate of I^- efflux without causing a corresponding increase in channel number and open probability. *2*) CFTR activation by PGF, but not by FSK, might cause a localized increase in cAMP near CFTR. This could allow PGF to stimulate CFTR with less total cellular cAMP. *3*) PGF could activate CFTR by a mechanism that involves the activation of both PKA and PKC. Because we were unable to observe an effect of extracellular K^+ on PGF-dependent I^- efflux and the sites of in vivo CFTR phosphorylation with FSK and PGF differ, it is most likely that CFTR activation by PGF involves stimulation of another kinase other that PKA. On the basis of the similarities among PGF- and PMA-dependent channel activation, in vivo phosphorylation, and inhibition by kinase-selective inhibitors, it is most likely that PGF-dependent CFTR activation involves PKC.

This study demonstrates CFTR activation by both PKC- and PKA-dependent signal transduction pathways and demonstrates that when both kinases are activated there is an additive effect on CFTR activity. The additive effects of PKA and PKC may be relevant to in vivo channel activation, where cells are likely to be stimulated by several agonists that, in concert, activate multiple signal transduction pathways. Our data also suggest that activation of PKC may amplify PKA-dependent stimulation at low cAMP levels. Such a mechanism may be important under physiological conditions in which submaximal levels of cAMP-dependent agonists produce less than maximal changes in intracellular cAMP. Recent studies have demonstrated CFTR activation by the PKC-dependent pathway in several mammalian tissues, including rabbit pancreatic acinar cells and guinea pig myocytes (7, 16). The effects of the combined activation of both signaling pathways on CFTR activity have not been described in these systems. Studies of CFTR activation by agonists, or agonist combinations, that activate several signal transduction pathways will lead to a better understanding of the in vivo function of this channel.

We thank Dr. Jonathan Cohn for providing us with access to data before publication and Sasikala Raman for expert technical assistance.

This work was supported by grants from the Cystic Fibrosis Foundation (K. A. Yurko-Mauro and W. W. Reenstra), Cystic Fibrosis Research (W. W. Reenstra), and the Nemours Foundation (W. W. Reenstra).

Address for reprint requests: W. W. Reenstra, Dept. of Clinical Science, Alfred I. duPont Hospital for Children, PO Box 269, Wilmington, DE 19899-0269.

Received 11 February 1998; accepted in final form 18 May 1998.

REFERENCES

1. **Anderson, M. P., H. A. Berger, D. P. Rich, R. J. Gregory, A. E. Smith, and M. J. Welsh.** Nucleoside triphosphates are required to open the CFTR chloride channel. *Cell* 67: 775–784, 1991.
2. **Berger, H. A., M. P. Anderson, R. J. Gregory, S. Thompson, P. W. Howard, R. A. Maurer, R. Mulligan, A. E. Smith, and M. J. Welsh.** Identification and regulation of the CFTR-generated chloride channel. *J. Clin. Invest.* 88: 1422–1431, 1991.
3. **Berger, H. A., S. M. Travis, and M. J. Welsh.** Regulation of the cystic fibrosis transmembrane conductance regulator Cl^- channel by specific protein kinases and protein phosphatases. *J. Biol. Chem.* 268: 2037–2047, 1993.
4. **Boyle, W. J., P. van der Geer, and T. Hunter.** Phosphopeptide mapping and phosphoamino acid analysis by two-dimensional separation on thin-layer cellulose plates. In: *Methods in Enzymology,* edited by T. Hunter and B. M. Sefton. San Diego, CA: Academic, 1991, vol. 201, p. 110–127.
5. **Cheng, S. H., D. P. Rich, J. Marshall, R. J. Gregory, M. J. Welsh, and A. E. Smith.** Phosphorylation of the R domain by cAMP-dependent protein kinase regulates the CFTR chloride channel. *Cell* 66: 1027–1036, 1991.
6. **Cleveland, D. W., S. C. Fischer, M. W. Kirschner, and U. K. Laemmli.** Peptide mapping by limited proteolysis in sodium dodecyl sulfate and analysis by gel electrophoresis. *J. Biol. Chem.* 252: 1102–1106, 1977.
7. **Collier, M. L., P. C. Levesque, J. L. Kenyon, and J. R Hume.** Unitary Cl^- channels activated cytoplasmic Ca^{2+} in canine ventricular myocytes. *Circ. Res.* 78: 936–944, 1996.
8. **Dechecchi, M. C., A. Tamanini, G. Berton, and G. Cabrini.** Protein kinase C activates chloride conductance in C127 cells stably expressing the cystic fibrosis gene. *J. Biol. Chem.* 268: 11321–11325, 1993.
9. **Dulhanty, A. M., and J. R. Riordan.** Phosphorylation by cAMP-dependent protein kinase causes a conformational change in the R domain of the cystic fibrosis transmembrane conductance regulator. *Biochemistry* 33: 4072–4079, 1994.
10. **Gadsby, D. C., and A. C. Nairn.** Regulation of CFTR channel gating. *Trends Biochem. Sci.* 19: 513–518, 1994.

Downloaded from journals.physiology.org/journal/ajpcell (065.021.193.086) on March 14, 2022.

11. **Gusovsky, F.** Prostaglandin receptors in NIH3T3 cells: coupling of one receptor to adenylate cyclase and of a second receptor to phospholipase C. *Mol. Pharmacol*. 40: 633–638, 1991.
12. **Hwang, T. C., M. Horie, and D. C. Gadsby.** Functionally distinct phospho-forms underlie incremental activation of protein kinase-regulated Cl^- conductance in mammalian heart. *J. Gen. Physiol*. 101: 629–650, 1993.
13. **Hwang, T. C., G. Nagel, A. C. Nairn, and D. C. Gadsby.** Regulation of the gating of cystic fibrosis transmembrane conductance regulator Cl channels by phosphorylation and ATP hydrolysis. *Proc. Natl. Acad. Sci. USA* 91: 4698–4702, 1994.
14. **Illek, B., H. Fischer, G. F. Santos, J. H. Widdicombe, T. E. Machen, and W. W. Reenstra.** cAMP-independent activation of CFTR Cl channels by the tyrosine kinase inhibitor genistein. *Am. J. Physiol*. 268 (*Cell Physiol*. 37): C886–C893, 1995.
15. **Jia, Y., C. J. Mathews, and J. W. Hanrahan.** Phosphorylation by protein kinase C is required for acute activation of cystic fibrosis transmembrane conductance regulator by protein kinase A. *J. Biol. Chem*. 272: 4978–4984, 1997.
16. **Kopelman, H., E. Ferretti, C. Gauthier, and P. R. Goodyer.** Rabbit pancreatic acini express CFTR as a cAMP-activated chloride efflux pathway. *Am. J. Physiol*. 269 (*Cell Physiol*. 38): C626–C631, 1995.
17. **Linsdell, P., and J. W. Hanraha.** Disulphonic stilbene block of cystic fibrosis transmembrane conductance regulator Cl^- channels expressed in a mammalian cell line and its regulation by a critical pore residue. *J. Physiol. (Lond.)* 496: 687–693, 1996.
18. **Nakao, A., T. Watanabe, S. Taniguchi, M. Nakamura, Z. I. Honda, T. Shimizu, and K. Kurokawa.** Characterization of prostaglandin $F_{2\alpha}$ receptor of mouse 3T3 fibroblasts and its functional expression in *Xenopus laevis* oocytes. *J. Cell. Physiol*. 155: 257–264, 1993.
19. **Picciotto, M. R., J. A. Cohn, G. Bertuzzi, P. Greengard, and A. C. Nairn.** Phosphorylation of the cystic fibrosis transmembrane conductance regulator. *J. Biol. Chem*. 267: 12742–12752, 1992.
20. **Reenstra, W. W., K. Yurko-Mauro, A. Dam, S. Raman, and S. Shorten.** CFTR chloride channel activation by genistein: the role of serine/threonine protein phosphatases. *Am. J. Physiol*. 271 (*Cell Physiol*. 40): C650–C657, 1996.
21. **Rich, D. P., H. A. Berger, S. H. Cheng, S. M. Travis, M. Saxena, A. E. Smith, and M. J. Welsh.** Regulation of the cystic fibrosis transmembrane conductance regulator Cl^- channel by negative charge in the R domain. *J. Biol. Chem*. 268: 20259–20267, 1993.
22. **Riordan, J. R., J. M. Rommens, B. S. Kerem, N. Alon, R. Rozmahel, Z. Grzelczak, J. Zielenski, S. Lok, N. Plavsic, J. L. Chou, M. L. Drumm, M. C. Iannuzzi, F. S. Collins, and L. C. Tsui.** Identification of the cystic fibrosis gene: cloning and characterization of complementary DNA. *Science* 245: 1066–1073, 1989.
23. **Smith, P. K., R. I. Krohn, G. T. Hermanson, A. K. Mallia, F. H. Gartner, M. D. Provenzano, E. K. Fujimoto, N. M. Goeke, B. J. Olson, and D. C. Klenk.** Measurement of protein using bicinchoninic acid. *Anal. Biochem*. 150: 76–85, 1985.
24. **Tabcharani, J. A., X.-B. Chang, J. R. Riordan, and J. W. Hanrahan.** Phosphorylation-regulated Cl^- channel in CHO cells stably expressing the cystic fibrosis gene. *Nature* 352: 628–631, 1991.
25. **Venglarik, C. J., R. J. Bridges, and R. A. Frizzell.** A simple assay for agonist-regulated Cl and K conductances in salt-secreting epithelial cells. *Am. J. Physiol*. 259 (*Cell Physiol*. 28): C358–C364, 1990.
26. **Watanabe, T., H. Satoh, M. Togoh, S. Taniguchi, Y. Hashimoto, and K. Kurokawa.** Positive and negative regulation of cell proliferation through prostaglandin receptors in NIH-3T3 cells. *J. Cell. Physiol*. 169: 401–409, 1996.
27. **Wilkinson, D. J., T. V. Strong, M. K. Mansoura, D. L. Wood, S. S. Smith, F. S. Collins, and D. C. Dawson.** CFTR activation: additive effects of stimulatory and inhibitory phosphorylation sites in the R domain. *Am. J. Physiol*. 273 (*Lung Cell. Mol. Physiol*. 17): L127–L133, 1997.

Downloaded from journals.physiology.org/journal/ajpcell (065.021.193.086) on March 14, 2022.